Cement and Concrete Composites 70 (2016) 98–109

Contents lists available at ScienceDirect

Cement and Concrete Composites

journal homepage: www.elsevier.com/locate/cemconcomp

Effect of loading rates on pullout behavior of high strength steel fibers embedded in ultra-high performance concrete

Man Xu, Bryan Hallinan, Kay Wille*

University of Connecticut, USA

ARTICLE INFO

Article history:
Received 28 July 2014
Received in revised form
12 June 2015
Accepted 26 March 2016
Available online 7 April 2016

Keywords:
Ultra high performance concrete
High strength fiber
Bond behavior
Pull out
Dynamic impact factor
Fiber embedment angle

ABSTRACT

In this paper single fiber pull-out performance of high strength steel fibers embedded in ultra-high performance concrete (UHPC) is investigated. The research emphasis is placed on the experimental performance at various pullout rates to better understand the dynamic tensile behavior of ultra-high performance fiber reinforced concrete (UHP-FRC). Based on the knowledge that crack formation is strain rate sensitive, it is hypothesized that the formation of micro-splitting cracks and the damage of cement-based matrix in the fiber tunnel are mainly attributing to the rate sensitivity. Hereby, different pull-out mechanisms of straight and mechanically bonded fibers will be examined more closely. The experimental investigation considers four types of high strength steel fibers as follows: straight smooth brass-coated with a diameter of 0.2 mm and 0.38 mm, half end hooked with a diameter of 0.38 mm and twisted fibers with an equivalent diameter of 0.3 mm. Four different pull out loading rates were applied ranging from 0.025 mm/s to 25 mm/s. The loading rate effects on maximum fiber tensile stress, use of material, pullout energy, equivalent bond strength, and average bond strength are characterized and analyzed. The test results indicate that half-hooked fibers exhibit highest loading rate sensitivity of all fibers used in this research, which might be attributed to potential matrix split cracking. Furthermore, the effect of fiber embedment angles on the loading rate sensitivity of fiber pullout behavior is investigated. Three fiber embedment angles, 0°, 20°, and 45°, are considered. The results reveal that there is a correlation between fiber embedment angle and loading rate sensitivity of fiber pullout behavior.

1. Introduction

The bond behavior between fiber and cementitious matrix is a key property for the material performance of fiber reinforced concrete. Numerous studies have been carried out to investigate the interfacial bond property by single fiber pullout tests. Naaman and Najm [1], Banthia [2], Sujiravorakul [3], Robins et al. [4], Kim et al. [5], Cunha et al. [6] and Wille et al. [7] explored the different pullout mechanisms of straight, end-hooked, and twisted fibers embedded in high strength or ultra-high strength cementitious matrices.

Although studies on single fiber pullout behavior under quasi-static condition are comprehensive, only a few researches have been conducted tests under dynamic conditions. Gokoz and Naaman [8] investigated the effect of loading rate on the pullout behavior of three types of fibers, smooth steel, glass and polypropylene, in mortar at loading velocities varying from 0.042 mm/s to 3000 mm/s. They revealed that polypropylene fibers showed strong dependence on loading velocity whereas smooth steel fibers exhibited no obvious loading rate sensitivity, and concluded that the friction effect was insensitive to loading velocity. Bindiganavile and Banthia [9] investigated the pull out response of three types of polymeric fibers and one type of flat end steel fiber under impact loading. They concluded that bond strength of all fiber types is sensitive to loading rates. Banthia and Trottier [10] performed pullout tests on deformed steel fibers under static & dynamic conditions and concluded that deformed steel fibers exhibit higher pullout resistance under dynamic conditions. Kim et al. [5] investigated the loading rate effect on the pullout behavior of deformed steel fibers and concluded that twisted fiber shows more rate sensitivity than end-hooked fiber for matrix strength ranging from 28 MPa to 83 MPa. Their results show that the rate sensitive behavior of twisted fibers is dependent on matrix strength. Abu-Lebdeh et al. [11] investigated the rate dependency of deformed and smooth steel fibers embedded in matrices of

* Corresponding author.
E-mail address: kwille@engr.uconn.edu (K. Wille).

http://dx.doi.org/10.1016/j.cemconcomp.2016.03.014
0958-9465/

strength ranging from 43 MPa to 196 MPa. While their results show that smooth fibers are rate independent, the rate dependent pull out response of deformed fibers is influenced by the embedment length and the matrix strength.

To the best of the author's knowledge to date, there is no other comprehensive research published on single fiber pullout embedded in ultra-high performance matrix at various loading rates. Exploring the pullout performance of high strength steel fibers at various loading rates will help to better understand the dynamic tensile behavior of ultra-high performance fiber reinforced concrete (UHP-FRC).

2. Objectives

The objectives of this research are: 1) to evaluate and compare the effect of loading rates on the bond properties of brass-coated straight steel fibers and deformed steel fibers embedded in UHPC, 2) to investigate the effect of embedment angle on bond properties under different loading rates. Based on these objectives, fiber type, fiber embedment angle, and loading rate have been selected as variables in this research.

3. Background information and hypothesis

Fig. 1 illustrates the shape of different types of fibers and their bond mechanism during fiber pullout. While straight smooth fibers (S-fiber) develop their bond strength mainly due to adhesion and friction along the fiber surface, end-hooked fibers (H-fibers) and twisted fibers (T-fibers) develop their bond strength mainly due to mechanical bond at the fiber end and along the entire fiber length, respectively. Both mechanisms require plastic deformation to straighten the fiber. The increase in pull-out resistance of deformed H- or T-fibers in comparison to S-fibers is limited by the bending resistance of the end hook (pulley approach [12]) and by the torque resistance [3], respectively, assuming no fiber rupture or matrix damage.

The relationship between induced fiber tensile stress and pull out slip is summarized in Fig. 2. Based on the results in Refs. [1,3–6], Fig. 2a shows the typical stress-slip curve of high strength steel fibers (tensile strength of approximately 3000 MPa, 435 ksi) embedded in high strength matrix (strength of 55–60 MPa, 8–8.7 ksi). Comparable fibers embedded in ultra-high strength matrix (strength of 194 MPa, 28.1 ksi) show a significant higher induced fiber tensile stress during pull out and thus increased material utilization. This leads to the conclusion that the mechanical bond capacity of the H- and T-fiber through fiber straightening could not be fully utilized in the lower strength matrix. Local matrix failure, such as crushing and micro split cracking, might be the reason for the limitation of pullout capacity.

Based on the mechanical equations for H-fibers provided by Alwan et al. [12] and for T-fibers provided by Sujiravorakul [3], Wille [13] calculated the theoretical contribution due to friction and mechanical bond and concluded that the pullout capacity had been limited by matrix failure (see Fig. 3).

Based on the knowledge that crack formation is strain rate sensitive, it is hypothesized that the formation of micro-splitting cracks and the damage of cement-based matrix in the fiber tunnel are mainly attributing to the rate sensitivity of singly pulled out fibers. Herby, different pull-out mechanisms of straight and mechanically bonded fibers will be examined more closely.

3.1. Hypothesis of matrix failure through end-hooked fibers (H-Fibers)

Although deformed fibers and thus H-fibers are generally considered to be loading rate sensitive during single fiber pull out, the amount of sensitivity is varying in the literature [5,11]. The following hypothesis is provided to explain insignificant [5,11] and significant loading rate sensitivity (in Ref. [11] and in this research) of H-fibers. During H-fiber pull out local pressure is induced into the surrounding matrix near the bending points of the end-hook. In dependency of matrix strength, fiber tensile strength, fiber diameter and end-hook geometry (bending angle) matrix crushing and micro split cracking potentially occur in a localized area. If the fiber pressure leads to an excess of the matrix splitting tensile strength in-plane-split-cracking will potentially occur (Fig. 4). Split cracking has been visually observed by the authors in composite material subjected to direct tension or bending and has also been reported in Ref. [14]. If a large embedment length is used during pull out, such as 12.7 mm in Ref. [11] or 15 mm in Ref. [5], high matrix confinement might be provided counteracting the split cracking, and thus reducing the loading rate sensitivity. Small embedment length, such as 6.35 mm in Ref. [11] or 6.5 mm in Ref. [7], have been used to prevent fiber failure in very high strength matrix and to represent a more statistically relevant embedment length (1/4 of fiber length, length = 30 mm) in a fiber composite. Hereby, the matrix confinement at the crack face is significantly reduced and could lead to in-plane and out-of-plane split cracking (Fig. 4). This could potentially contribute to loading rate sensitivity of hooked fibers with short embedment length. Hence the embedment length of H-fibers influences the rate sensitivity. It is hypothesized that micro split cracking mainly contributes to the loading rate sensitivity of pulled out H-fibers. The amplitude of rate sensitivity depends on matrix strength, matrix confinement (thus embedment length), and fiber strength and geometry.

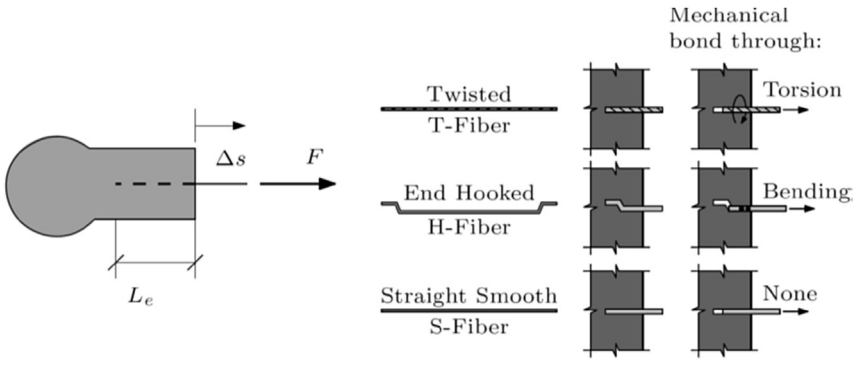

Fig. 1. Pull out mechanisms of straight, end-hooked, and twisted steel fibers.

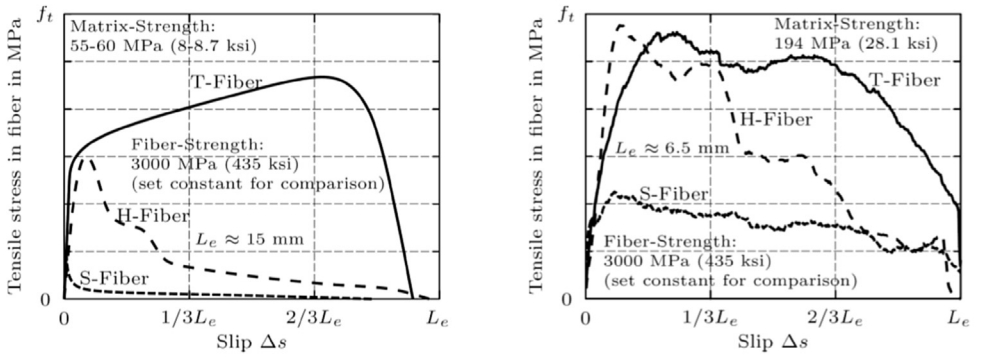

a) Embedded in high strength matrix, based on results in [1,3-6]

b) Embedded in ultra-high strength matrix, based on results in [7]

Fig. 2. Pull out behavior of high strength straight (S), end-hooked (H), and twisted (T) fibers embedded in a) high strength matrix and b) ultra-high strength matrix [1,3–7].

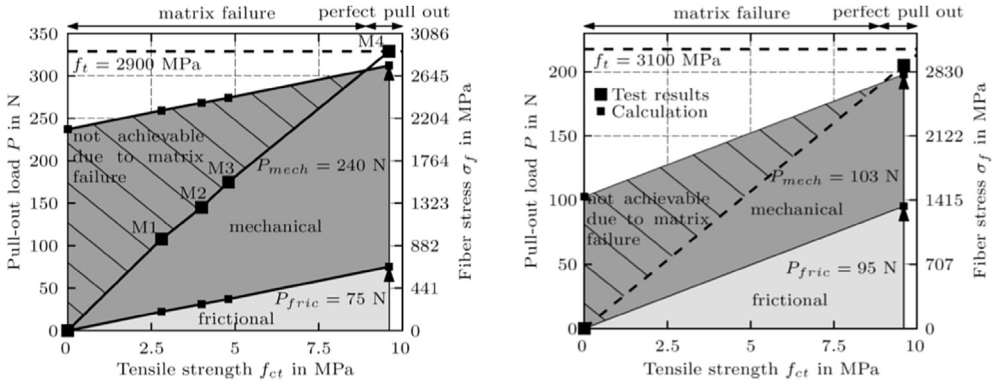

a) Pull-out capacity of hooked fiber [13]

b) Pull-out capacity of twisted fiber [13]

Fig. 3. Pull-out capacity and distinguished bond contribution of one single hooked (H-) fiber and twisted (T-) fiber embedded in cement based matrices of different compressive strength, and thus different tensile strength [13], embedment length = 6.5 mm.

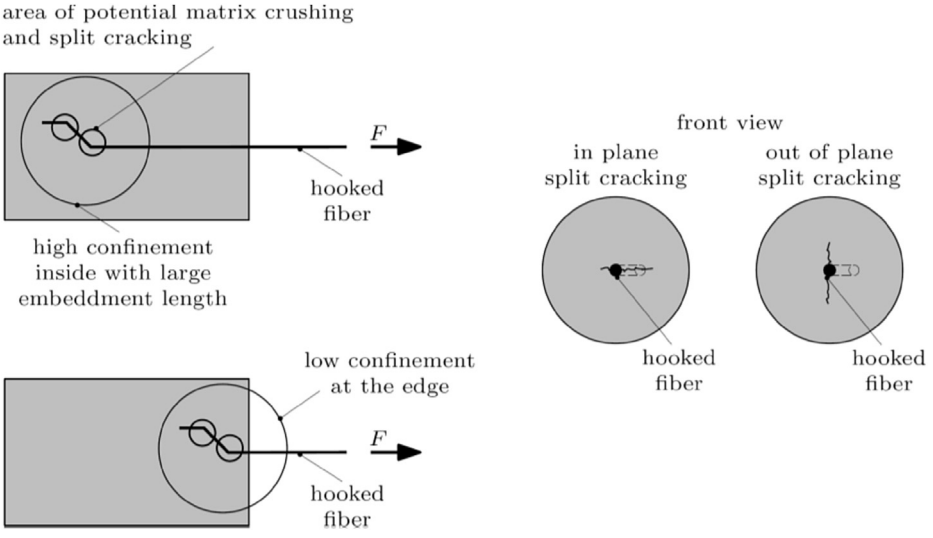

Fig. 4. Potential matrix failure during pull out of an end-hooked (H-) fiber.

3.2. Hypothesis of matrix failure through twisted fibers (T-Fibers)

The following hypothesis is provided to explain the variation of loading rate sensitivity of twisted fibers embedded in normal and high strength matrices [5] and in ultra-high strength matrix provided in this research. During T-fiber pull out shearing as well as torsional action induces local pressure along the embedded surface. In dependency of matrix strength, fiber tensile strength, fiber

diameter, cross-sectional shape and fiber twist ratio, matrix crushing and micro split cracking potentially occur in a localized area of the fiber tunnel (Fig. 5). Similar to reinforcing bars split cracking can potentially occur, when the mechanical bond is too strong for the surrounding matrix. It is hypothesized that shear forces can be transferred into the split cracked concrete over an active crack length of $\ell_{e,cr}$ until the split crack widens without significant shear force transfer. The active splitting crack length $\ell_{e,cr}$ travels towards the end of the fiber during pullout. Under dynamic loading the inertia effect of crack formation could lead to a higher matrix resistance and potentially increase $\ell_{e,cr}$, which would increase the loading rate sensitivity. In higher strength matrices the active crack length $\ell_{e,cr}$ might be longer due to the higher resistance of the matrix. Therefore it could be possible that twisted fibers show only slight loading rate sensitive behavior when these are embedded in a very high strength matrix with a short embedment length. Since under these conditions $\ell_{e,cr}$ might already been utilized until fiber end at quasi-static loading, $\ell_{e,cr}$ will not be able to further increase its length and thus its loading rate effect under dynamic conditions (Fig. 5). This might explain, why significant loading rate sensitivity is observed of single T-fibers pulled out from a low strength matrix with a large embedment length of 15 mm [5].

3.3. Straight smooth (S-Fibers)

Typically well aligned S-fibers pull out cleanly without crack formation or damage explaining the loading rate insensitivity observed by Gokoz and Naaman [8] or Banthia and Trottier [10]. Wille and Naaman [7,15] have conducted single fiber pullout tests of S-fibers embedded in UHPC under static conditions. With increase of matrix strength in excess of 200 MPa they observed that straight steel fibers display atypical pull out load slip-hardening behavior rather than a sharp load drop followed by a slip-softening behavior. This behavior has been attributed to the strong bond between matrix and fiber, leading to particle abrasion in the fiber tunnel, wedging of the particles, scratching the fiber surface and partly or full delamination of the brass-coating. Additionally, a small material nose at the fiber end, formed by the cutting process, anchors the fiber and might further scratch the matrix tunnel. Overall, a clean fiber pullout has not been observed in the prior research [7,15], which fuels the hypothesis that the pullout of straight fibers embedded in UHPC might be loading rate sensitive.

Based on the formulated hypotheses the research program will investigate the loading rate sensitive pullout behavior of S-, H- and T-fibers embedded in UHPC. Additionally, the pullout angle will be changed for selected series to investigate the effect of not well aligned fibers in the composite.

4. Experimental program

4.1. Effect of fiber types on the loading rate sensitivity of single fiber pullout

The pullout behavior of four types of high strength steel fibers is investigated at four different loading rates: 0.025 mm/s, 0.25 mm/s, 2.5 mm/s, and 25 mm/s. The test series include high strength (2600 MPa) brass-coated steel fibers with a diameter of 0.2 mm (S-0.2), a high strength (2900 MPa) straight steel fiber manufactured from cutting off a hooked fiber with a diameter of 0.38 mm (SH-0.38), a high strength (2900 MPa) half-hooked steel fiber with a diameter of 0.38 mm (HH-0.38), and a high strength (3100 MPa) low twisted steel fiber with an equivalent diameter of 0.3 mm (T-0.3). The production of the SH- and HH-fiber, the dimension of hooked fiber, and the embedment length are provided in Fig. 6. The commercially available hooked fiber was reduced to a half-hooked fiber to prevent fiber failure and the SH-fiber was used to provide reference performance. The T-fibers were self-manufactured from round wires with a pitch of 8 mm. The fiber pitch is defined as the length of one full twist (360°) about the longitudinal fiber axis. Information about fiber strength and fiber geometry is summarized in Table 1.

4.2. Effect of fiber embedment angles on loading rate sensitivity of single fiber pullout

The pullout behavior with respect to embedment angles is explored for SH-fiber series. Three fiber embedment angles, 0°, 20°, and 45°, each at two different loading rates, quasi-static condition (0.025 mm/s) and seismic condition (25 mm/s) are investigated.

Overall, the proposed experimental program includes six different test series under four loading rates and three to six specimens per mix, as summarized in Table 2. Each test is analyzed and discussed in the next section to characterize the effects of loading rates on the pullout mechanical parameters of fibers. The identification is defined to facilitate discussion: the first letter indicates the type of fiber, the first number denotes the fiber diameter in mm, and the last number indicates the fiber embedded angle. For example, SH-0.38-0 is a straight-hooked fiber with a diameter of 0.38 mm embedded at 0°.

4.3. Material and specimen preparation

The matrix used in this study is a self-consolidating ultra-high performance concrete (UHPC) with a 28 day compressive strength of 194 MPa under ambient curing conditions. The mix proportions and mechanical properties are summarized in Table 3. The interested reader is referred to [16,17] for further information about the

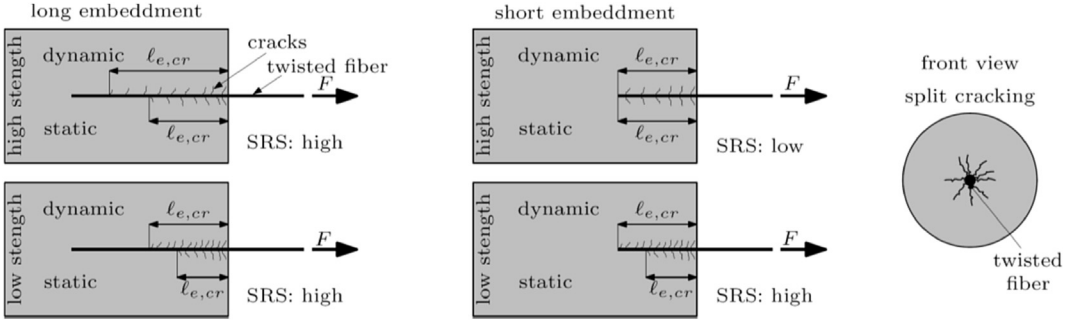

Fig. 5. Potential matrix failure during pull out of a twisted (T-) fiber.

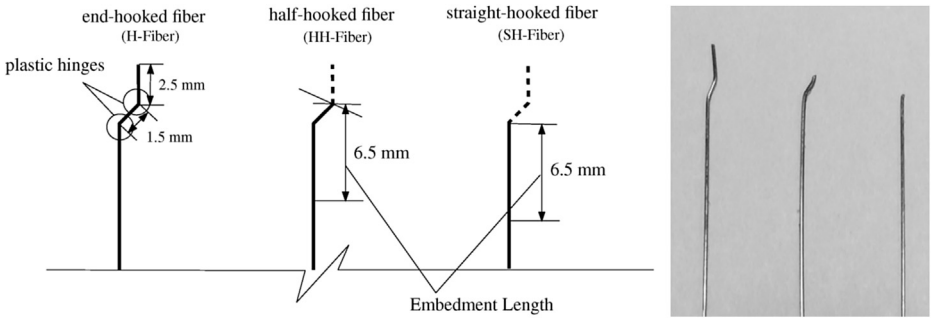

Fig. 6. The illustration of detail of HH-fibers and SH-fibers.

Table 1
Properties of fibers used in the study.

Notation	Form	Pitch	d_f	l_f	l_f/d_f	Tensile strength, f_s
		mm	mm	mm	–	MPa
S	Straight	–	0.20	13	65	≈2600
SH	Straight-hooked	–	0.38	30#	79	≈2900
HH	Half-hooked	–	0.38	30#	79	≈2900
T	Low twisted	8	0.30[a]	30	100	≈3100

[a] Manufactured out of round wire with d_f = 0.30 mm, shaped into prism a/b = 0.24/0.30 mm,[#] prior to cutting.

material mix development and characterization and referred to [7,15–19] for further information about mixing and specimen preparation procedures used in this research.

4.4. Test setup

Previous researches [5,7,15] have proved that the pullout test system can effectively capture the single fiber pullout behavior under quasi-static conditions. The same test setup (Fig. 7) is adopted for dynamic testing in this research. The pullout test system is comprised of a grip system (specimen grip system and fiber grip system), a MTS deformation controlled servo-hydraulic load frame, and a linear variable displacement transducer (LVDT) for vertical displacement measurement. The specimen is carefully positioned and held in the specimen grip system to avoid lateral confinement of the embedded fiber. The LVDT is then attached to the fiber grip system assuming to have a vertical displacement which is assumed to be equal to the fiber slip when elastic deformation of the fiber and specimen are neglected.

5. Analytical procedure for average curve

The experimentally obtained pullout load versus slip curves – at least three – are averaged within each series. The following mathematical method [20] has been used to guarantee the validity of the average curve (Fig. 8).

In step I the pullout load versus slip data is separated into two parts. The partition point is the maximum pull out load of the first ascending portion. In step II the test data are closely approximated by two polynomial curves (one for the first portion and one for the second portion) using least sum of squares errors data fitting function in MATLAB, *polyfit*. The two fitted curves of each test data are then partitioned into pieces of equal arc length in step III. For simplicity only 5 pieces are illustrated in Fig. 8, but the algorithm allows for any number depending on the degree of accuracy. However, the same number of pieces for each curve in one series is defined to provide the basis of calculating one single average curve (step IV). After partitioning each newly created point of same number is used to calculate the x- and y-coordinate for the average curve in step V. This process produces an accurate representation of the average curve, the overall shape and the maximum value. Fig. 8 includes a simplified sample of incorrect averaging. Here it can be seen that by averaging the y-values of each curve at same x-values an average curve is produced, which does not represent correctly

Table 2
Single fiber pullout test series investigated in this study.

Type of fiber	Diameter (mm)	Angle (°)	Load rates (mm/s)
S	0.2	0	0.025
			0.25
			2.5
			25
SH	0.38	0	0.025
			0.25
			2.5
			25
		20	0.025
			25
		45	0.025
			25
HH	0.38	0	0.025
			0.25
			2.5
			25
T	0.3	0	0.025
			0.25
			n/a
			25

Table 3
Mixture proportions by weight for UHPC.

Type	UHPC
Cement	1
Silica Fume	0.25[a]
Glass Powder	0.25
Water[b]	0.22
Superplasticizer[c]	0.0054
Fiber	0
Sand A[d]	0.28
Sand B[e]	1.10
Sand A/B	20/80
f_c(MPa)[f]	194
d_{sp} (mm)[g]	296

[a] Silica fume (d_{50} = 0.4 μm).
[b] Total water.
[c] Solid content.
[d] Silica sand d_{max} = 0.2 mm.
[e] Silica sand d_{max} = 0.8 mm.
[f] cubic concrete at 28 days age (a = 50 mm).
[g] spread value on flow table in accordance with ASTM C230/C230M.

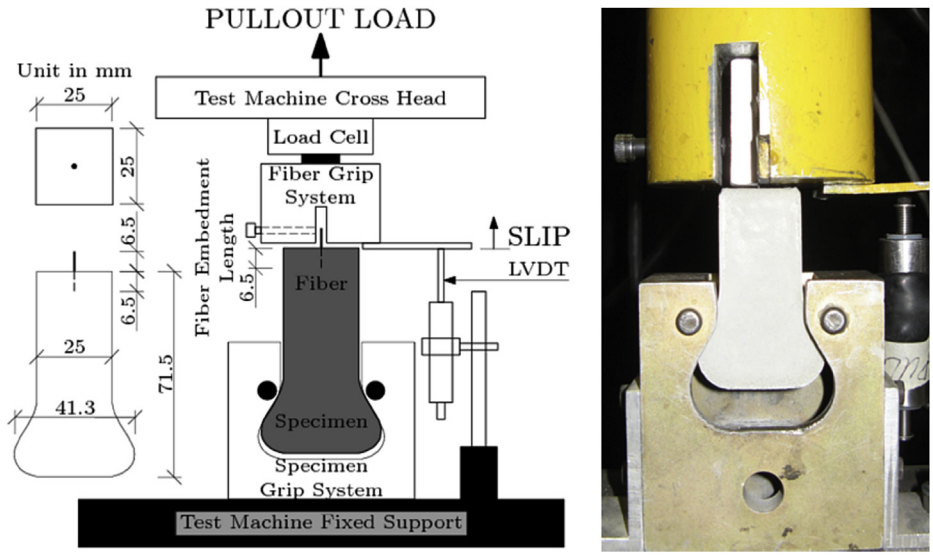

Fig. 7. Pullout specimen and test setup [5,7,15].

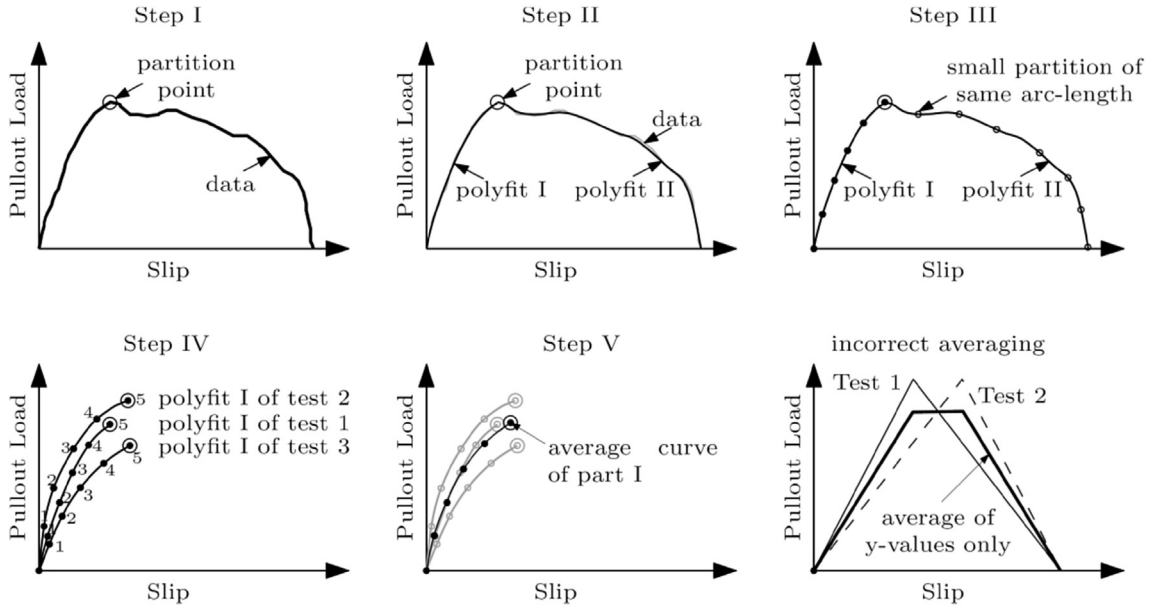

Fig. 8. Illustration of method to average several pullout load versus slip curves.

the sharp peak of the two exemplified curves, by showing an incorrect plateau. This artificial representation particularly occurs, when the peak values are shifted on the x-axis.

6. Test results and discussion

In pursuit of the two main research objectives the following mechanical parameters are investigated in terms of their loading rate sensitivity: pullout load (P) versus slip (s) curve, the maximum pullout load (P_{max}), the maximum fiber tensile stress ($\sigma_{f,max}$), the fiber material utilization (defined as $\sigma_{f,max}/f_s$), pullout energy (W_p), the equivalent bond strength (τ_{eq}), and the average bond strength (τ_{av}). The equations for these parameters are provided in Ref. [7]. For each mechanical parameter the corresponding dynamic impact factor (DIF), which is the ratio of dynamic response to static response (0.025 mm/s), is calculated to signify the loading rate effect.

6.1. Effect of fiber type

Based on the analytical procedure for the average curve illustrated above, average pullout load versus slip curves of the four fiber type series under four different loading rates are shown in Figs. 9–12.

From Figs. 9 to 12, it can be seen that the pullout behavior of fibers embedded in UHPC under quasi-static conditions is preserved under increased loading rates, especially the pronounced atypical load-slip behavior of S-fibers (Figs. 9 and 10). HH-fiber series resisted the largest pullout load due to mechanical anchorage and largest fiber diameter, followed by T-fiber series, SH-fiber series and S-fiber series. Maximum pullout loads of each test series at each loading rate and corresponding DIFs are calculated

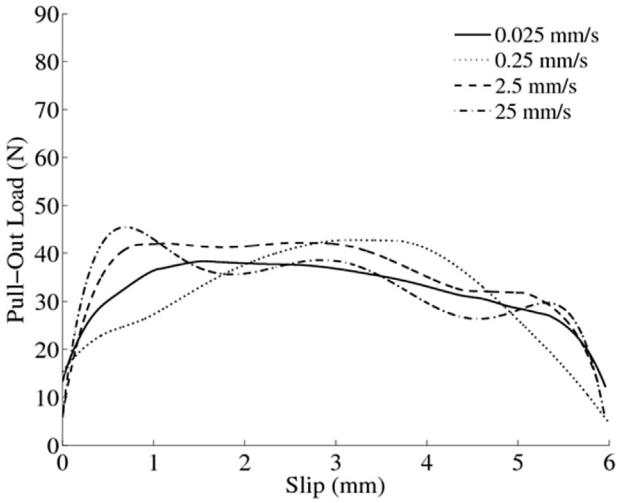

Fig. 9. Pullout load versus slip of S-0.2-0.

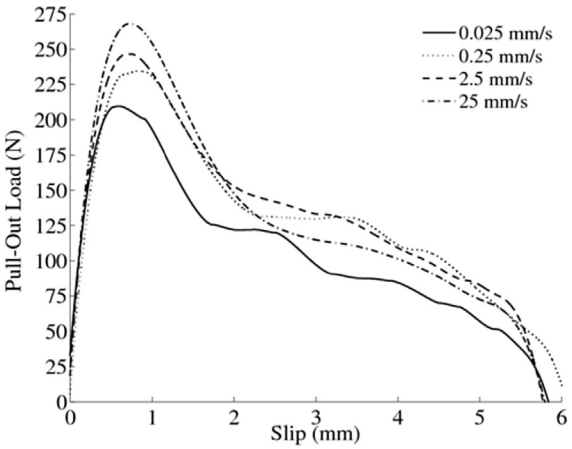

Fig. 11. Pullout load versus slip of HH-0.38-0.

and summarized in Table 4.

The atypical pullout load versus slip behavior of straight fibers in Figs. 9 and 10 results from the optimized particle packing of ultra-high strength matrix, which leads to significantly greater bond strength as introduced in Ref. [15]. Moreover, S-fiber series show slight loading rate sensitivity. The maximum pullout load is 38 N at quasi-static condition (0.025 mm/s) and increases to 46 N at seismic condition (25 mm/s), yielding to a corresponding DIF of 1.19. This rate sensitivity might be attributed to matrix abrasion, fiber surface damage and minimal fiber end anchorage [15].

Since SH-fibers are self-manufactured from end-hooked fibers by cutting all plastic hinges at the hook, they exhibit similar bond-slip behavior as straight fibers, but at a larger pullout load due to the larger fiber diameter (see Fig. 10). There is no noticeable loading rate sensitive behavior of SH-fiber series. The maximum pullout loads at loading rates of 0.025 mm/s, 0.25 mm/s, 2.5 mm/s, and 25 mm/s are 131 N, 137 N, 140 N, and 132 N, respectively. These values have corresponding DIFs of 1.04, 1.07, and 1.01, all of which are negligible and demonstrate that SH-fibers can be considered loading rate insensitive. Comparing the load rate sensitive behavior between SH-fiber (d = 0.38 mm) and S-fiber (d = 0.2 mm) suggests that decrease in diameter increase the rate sensitivity of straight fiber embedded in ultra-high strength matrix.

HH-fibers are self-manufactured from end-hooked fibers by cutting one plastic hinge at the hook, which alters the mechanical bond of the original end-hooked fiber with two plastic hinges. The change in mechanical bond and thus load capacity can be observed in a comparison of Fig. 3a (75 N friction + 240 N mechanical bond for two hinges = 315 N load capacity) and Fig. 11 (75 N friction + 120 N mechanical bond for one hinge = 195 N load capacity). It should be noted that after the mechanical bond for HH-fibers is overcome, that is, the hook is straightened upon loading; the pullout load is convergent with the values of SH-fibers. The HH-fiber series exhibit a significant loading rate sensitive behavior. The maximum pullout load is 209 N at quasi-static condition (0.025 mm/s) and increases to 268 N at seismic condition (25 mm/s), resulting in a DIF of 1.28. This load rate sensitivity supports the hypothesis of potential local micro-split cracking due to the high tensile strength of the fiber, high local anchorage and short embedment length. The inertia effect of micro-split crack formation could lead to a higher matrix resistance and thus increased pull out load at increased pull out rate.

For T-fibers used in here the pullout load capacity increases with increasing of loading rates. The maximum pullout load is 171 N at quasi-static condition (0.025 mm/s) and increases to 183 N and 195 N at a loading rate of 0.25 mm/s and 25 mm/s, respectively,

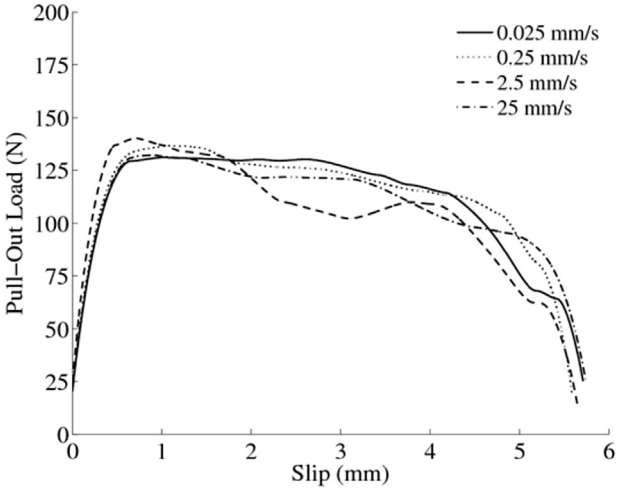

Fig. 10. Pullout load versus slip of SH-0.38-0.

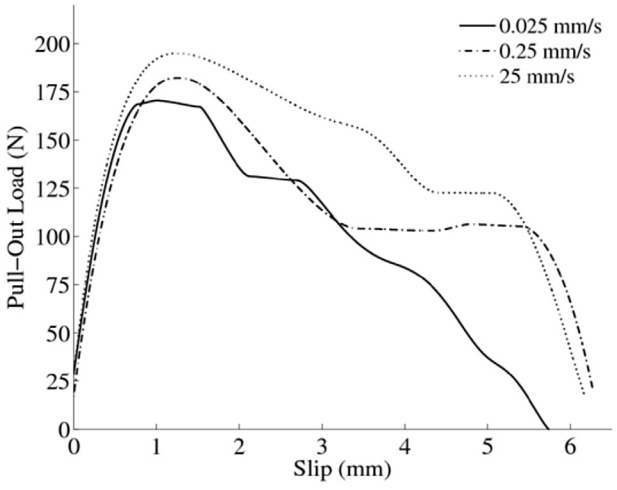

Fig. 12. Pullout load versus slip of T-0.3-0.

Table 4
Loading rate effect on the mechanical parameter of fiber pullout.

Notation	Angle	Loading rate	P_{max}	DIF	σ_{max}	DIF	σ_{max}/f	DIF	W_p	DIF	τ_{eq}	DIF	τ_{av}	DIF
	°	mm/s	N	–	MPa	–	–	–	N mm	–	MPa	–	MPa	–
S20	0	0.025	38.3	1.00	1221	1.00	0.47	1.00	195.0	1.00	15.2	1.00	9.5	1.00
		0.25	42.8	1.12	1363	1.12	0.52	1.12	192.1	0.98	14.9	0.98	10.6	1.12
		2.5	42.2	1.10	1343	1.10	0.52	1.10	215.3	1.10	16.7	1.10	10.5	1.10
		25	45.5	1.19	1448	1.19	0.56	1.19	201.6	1.03	15.7	1.03	11.3	1.19
SH38	0	0.025	131.0	1.00	1156	1.00	0.40	1.00	656.2	1.00	28.6	1.00	17.7	1.00
		0.25	136.7	1.04	1205	1.04	0.42	1.04	651.2	0.99	28.4	0.99	18.5	1.04
		2.5	140.2	1.07	1236	1.07	0.43	1.07	621.7	0.95	27.1	0.95	18.9	1.07
		25	132.1	1.01	1165	1.01	0.40	1.01	625.5	0.95	27.3	0.95	17.8	1.01
	20	0.025	128.8	1.00	1136	1.00	0.39	1.00	523.2	1.00	22.8	1.00	17.4	1.00
		25	158.3	1.23	1396	1.23	0.48	1.23	629.6	1.20	27.4	1.20	21.4	1.23
	45	0.025	143.7	1.00	1267	1.00	0.44	1.00	500.6	1.00	21.8	1.00	19.4	1.00
		25	152.4	1.06	1344	1.06	0.46	1.06	516.6	1.03	22.5	1.03	20.6	1.06
HH38	0	0.025	209.4	1.00	1847	1.00	0.64	1.00	629.9	1.00	25.8	1.00	27.4	1.00
		0.25	234.6	1.12	2069	1.12	0.71	1.12	731.5	1.16	29.9	1.16	30.7	1.12
		2.5	246.6	1.18	2174	1.18	0.75	1.18	795.1	1.26	32.5	1.26	32.3	1.18
		25	268.1	1.28	2364	1.28	0.82	1.28	779.3	1.24	31.9	1.24	35.1	1.28
T30	0	0.025	170.5	1.00	2412	1.00	0.78	1.00	626.6	1.00	31.5	1.00	27.8	1.00
		0.25	182.2	1.07	2578	1.07	0.83	1.07	759.6	1.21	38.2	1.21	29.7	1.07
		25	195.0	1.14	2759	1.14	0.89	1.14	895.1	1.43	45.0	1.43	31.8	1.14

resulting in a corresponding DIF of 1.07 and 1.14. These results are in similar range as the results in Ref. [5] in which a DIF of 1.11 and 1.18 was reported for a twisted fiber embedded 15 mm in a matrix with strength of 83 MPa and pulled out at similar loading rates. The results suggest that the inertia effect of crack formation could potentially increase $\ell_{e,cr}$ (Fig. 5), which would increase the loading rate sensitivity and thus the pull out load. Comparing the load rate sensitive behavior of twisted fibers also suggests that decrease of embedment length and increase in matrix strength decreases the rate sensitivity.

6.1.1. Influence on maximum fiber tensile stress

The maximum fiber tensile stress ($\sigma_{f,\ max}$) is used to evaluate the mechanical bond contribution and calculated based on maximum pullout load ($P_{\max}$) and fiber diameter. Results in Fig. 13a and Table 4 reveal that T-fiber series exhibit the largest maximum fiber tensile stress under each loading rate, followed by the HH-fiber series, S-series, and SH-fiber series. The maximum fiber tensile stresses are 2412 MPa, 1847 MPa, 1221 MPa, 1156 MPa at quasi-static loading rate, and 2759 MPa, 2364 MPa, 1448 MPa, 1165 MPa at seismic loading rate for T-fibers, HH-fibers, S-fibers and SH-fibers, respectively. The maximum tensile stresses of T-fiber and HH-fiber are approximately twice the stress of S-fibers under both quasi-static and seismic conditions. It is concluded that the mechanical bond of deformed fibers significantly improves the pullout performance of high strength steel fiber embedded in UHPC, consequently, the potential tensile behavior of UHP-FRC under various loading rates.

The dynamic impact factor for $\sigma_{f,\ max}$ of different fiber types are summarized in Fig. 13d and Table 4. Among the four fiber types, HH-fiber series exhibit strongest loading rate dependence with a maximum DIF of 1.28 at 25 mm/s loading rate. Comparatively, the increasing trend for the S-fiber and T-fiber series are less pronounced, with a maximum DIF of 1.19 and 1.14 at 25 mm/s loading rate, respectively. The SH-fiber series has little variance for DIFs of $\sigma_{f,\ max}$, and is considered to have no loading rate dependency.

6.1.2. Influence on the material use of fiber

Material use of fiber herein is defined as the maximum induced fiber tensile stress, $\sigma_{f,max}$, divided by fiber tensile strength, f_s , and is indicative of fiber efficiency [7]. The results in Table 4 and Fig. 13b illustrate the loading rate effect on material use. The T-fiber series exhibit the largest material use at each loading rate, approximately 80% of the total fiber strength is used during pullout, which is twice that of S-fibers. Since material use ($\sigma_{f,max}/f_s$) is directly proportional to $\sigma_{f,max}$, the same loading rate sensitivity behavior as $\sigma_{f,max}$ is observed in Fig. 13d.

6.1.3. Influence on the average bond strength

The average bond strength (τ_{av}) facilitates the comparison and analysis between different specimen series when the maximum pullout load happens at different slip. Therefore, the average bond strength is calculated based on the maximum pullout load and fiber embedded length [7]. The value of average bond strength and corresponding DIFs are shown in Table 4 and plotted in Fig. 13c. T-fibers and HH-fibers display a stronger bond behavior at every loading rate. τ_{av} of deformed fibers (T-fiber and HH-fiber) is nearly three times that of S-fibers. Since τ_{av} is proportional to $\sigma_{f,\ max}$, the same loading rate sensitivity behavior as $\sigma_{f,\ max}$ is observed in Fig. 13d.

6.1.4. Influence on the maximum pullout energy

Pullout energy (W_p) is defined geometrically by the integral of the area of pullout load versus slip curve. The loading rate effect on W_p is shown in Fig. 14a and Table 4. Fig. 14a illustrates that deformed fibers (T-fiber and HH-fiber) are consistently more resistant than straight fibers in pullout test across all loading rates. The higher W_p of SH-fibers than S-fibers is due to the larger pullout loads. In general, the values presented in Table 4 and Fig. 14c suggest that the loading rate has a greater impact on pullout energy than maximum fiber tensile stress or maximum pull out load. The inertia effect of micro-crack formation potentially increases the fiber matrix bond not only at the onset of fiber pullout, but also during the pullout. This would amplify the load rate sensitivity of the pullout energy. HH-fiber series express loading rate sensitivity on pullout energy with 630 Nmm at quasi static loading rate and 780 Nmm at seismic loading rate, resulting in a corresponding DIF of 1.24. For T-fibers the loading rate effect on W_p is more noticeable than maximum fiber tensile stress. The pullout energy is 627 Nmm, 760 Nmm and 895 Nmm, for 0.025 mm/s, 0.25 mm/s and 25 mm/s, leading to a DIF of 1.21 and 1.43, respectively. In a comparison to the deformed fibers, straight fibers (S-fiber and SH-fiber) do not show obvious loading rate sensitivity on pullout energy due to the smaller variation of DIFs.

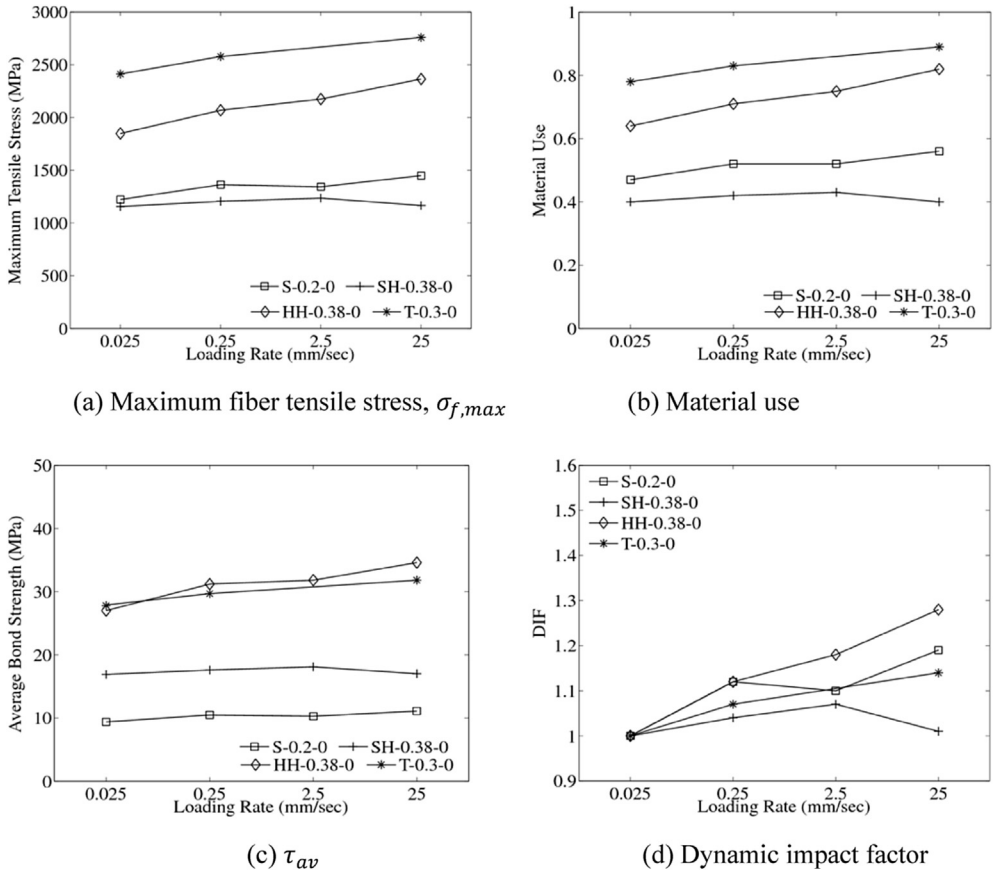

Fig. 13. Loading rate effect on maximum fiber tensile stress, material use, and τ_{av}.

6.1.5. Influence on the equivalent bond strength

The equivalent bond strength (τ_{eq}) reflects the average bond strength during pullout calculated based on the pullout energy W_p and fiber embedded length [5,7]. The behaviors of equivalent bond strength for each fiber type are shown in Table 4 and Fig. 14b. The T-fiber, HH-fiber and SH-fiber series display a greater equivalent bond strength than S-fiber series at each loading rate, which further reinforces that the fiber types with both mechanical bond and frictional effect significantly improves bond behavior. The τ_{eq} of T-fibers, HH-fibers and SH-fibers is approximately twice to three times of that of S-fibers. Since τ_{eq} is proportional to W_p, the same loading rate sensitivity behavior as W_p is observed in Fig. 14c.

6.2. Effect of fiber embedment angle

In practical applications, the fiber orientation is random and the results of pullout behavior of fiber aligned with the direction of load are not representative. Therefore, investigating the pullout performance based on fiber embedment angles is significant. Researchers have concluded that fiber embedment angle indeed affects the fiber pullout behavior at quasi-static condition. V.C. Li et al. [21] suggested that pullout load and energy increase with the increase of fiber inclination, but limited to given angle due to the matrix spalling. Yun Lee et al. [22] investigated five inclination angles embedded in an ultra-high strength matrix and observed that the maximum pullout load occurs between 30° and 45 embedment angles. In this research, the authors investigate load rate sensitivity of SH-fibers embedded at 0°, 20°, and 45°. Specimen preparation and test setups for fibers with embedment angles of 20° and 45° are illustrated in Fig. 15. Two loading rates are considered: 0.025 mm/s represents quasi-static condition and 25 mm/s denotes the seismic condition.

Fig. 16 shows the permanent deformation of the embedded fiber parts after pull-out. These deformations were consistence over all series and loading rates and indicate the plastic deformation during pull out of inclined steel fibers. The same mechanical parameters are investigated as previous discussions, the pullout load (P) versus slip (s) curve, the maximum fiber tensile stress ($\sigma_{f,max}$), the material use, the pullout energy (W_p), the equivalent bond strength (τ_{eq}), and the average bond strength (τ_{av}). These values and the corresponding DIFs are shown in Table 4. β_θ is defined herein to indicate the fiber embedment angle effect on loading rate sensitive behavior. It is calculated as follows:

$$\beta_\theta = \frac{(DIF_\theta - DIF_{\theta_0})}{DIF_{\theta_0}} * 100\% \quad (1)$$

where DIF_θ is the dynamic impact factor at a θ embedment angle; DIF_{θ_0} is the dynamic impact factor at 0° embedment angle.

As depicted in Fig. 17, the maximum pullout loads for 0°, 20°, 45° embedment angles are 131.0 N, 128.8 N, 143.7 N at the quasi-static loading rate and 132.1 N, 158.3 N, 152.4 N at the seismic loading rate, resulting in the DIFs as 1.01, 1.23, 1.06, respectively. Therefore, it is concluded that fibers embedded at 0° embedment angle have no loading rate sensitivity, whereas 20° and 45° embedment angle series exhibit significant and slight loading rate sensitive behaviors, respectively. Based on Eq. 1, β_{20° is 22% and β_{45° is 5%. A 20° embedment angle increases the loading rate effect by more than 20%. It reveals that the loading rate effects on fiber pullout behavior are dependent on fiber embedment angle and might be attributed

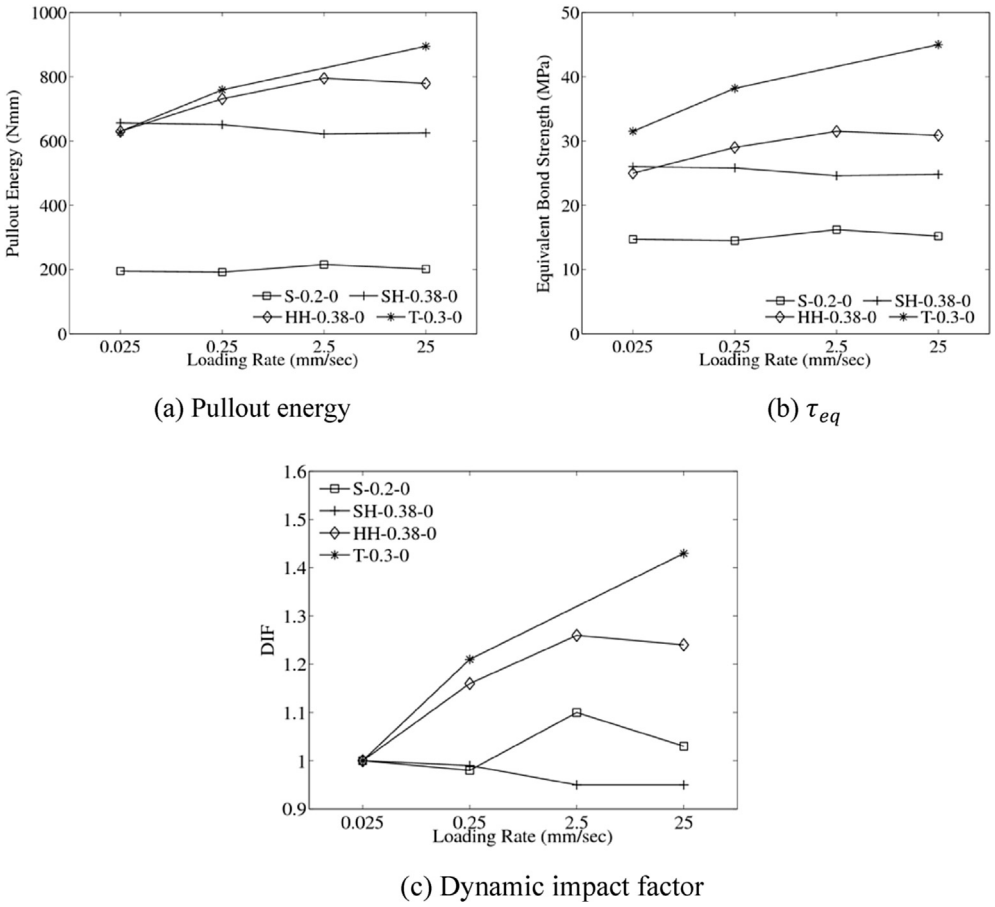

Fig. 14. Loading rate effect on pullout energy and τ_{eq}.

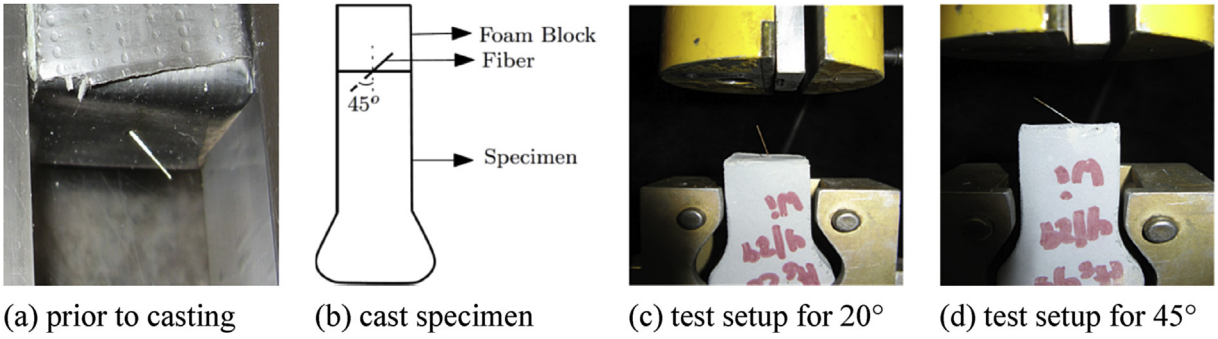

Fig. 15. Illustration of mold preparation and test setups for the fiber with embedment angles.

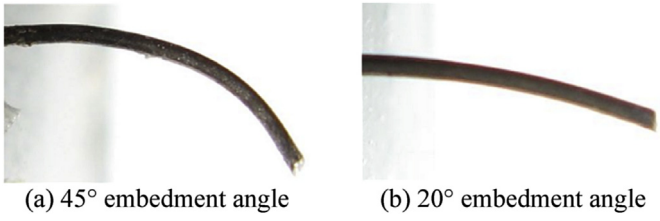

Fig. 16. Embedded fiber parts after pulled out from matrix.

to the matrix damage.

The results of loading rate effect on maximum fiber tensile stress, material use and average bond strength under different fiber embedment angles are summarized in Table 4 and plotted in Fig. 18. SH-0.38-20 shows the highest loading rate sensitive behavior with a DIF of 1.23 at a loading rate of 25 mm/s. As previously concluded SH-0.38-0 is considered to be loading rate insensitive. Based on the Eq. (1), β_{20° is 22% and β_{45° is 5%. Therefore, a 20° embedment angle increases the loading rate effect on maximum fiber tensile stress, material use and average bond strength by more than 20%.

Fig. 19 shows the loading rate effect on pullout energy and equivalent bond strength for different fiber embedment angles. The

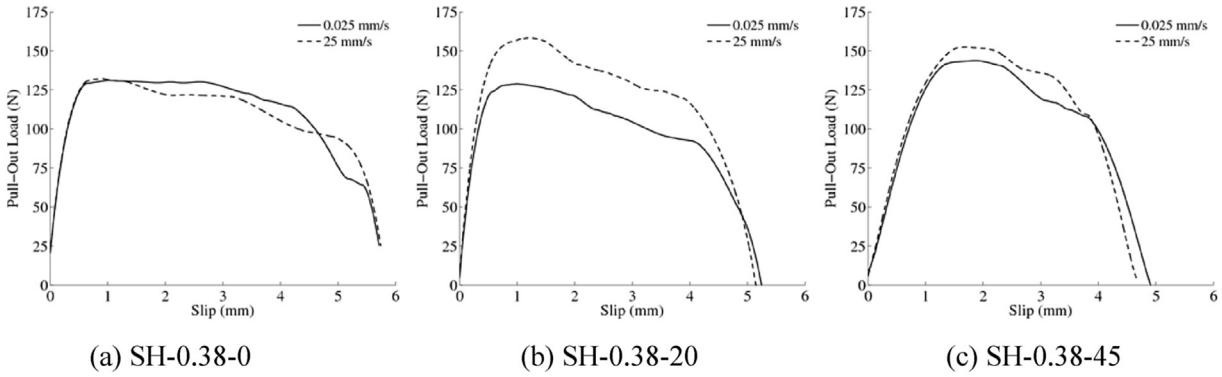

Fig. 17. Pullout load versus slip of SH-fibers with different embedment angles.

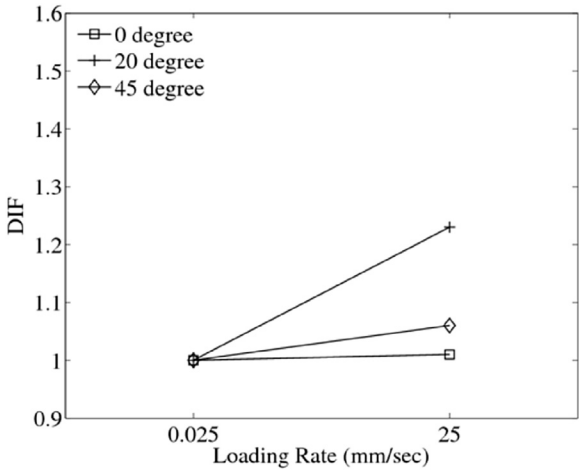

Fig. 18. Loading rate effect on maximum fiber tensile stress, material use and τ_{av}.

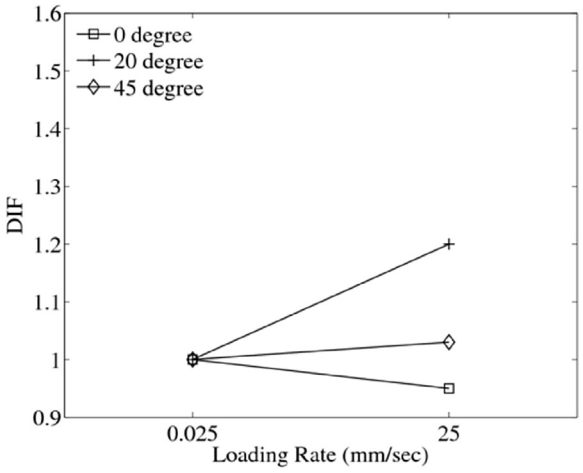

Fig. 19. Loading rate effect on pullout energy and τ_{eq}.

results and the corresponding DIFs are computed and summarized in Table 4. Similarly, SH-0.38-20 exhibits significant loading rate sensitivity on pullout energy and τ_{eq} with a DIF of 1.20 at the seismic loading rate. Based on the Eq. (1), β_{20° is 26% and β_{45° is 8%. Once again, a 20° embedment angle amplifies the loading rate effect on pullout energy and equivalent bond strength.

7. Summary & conclusion

This research investigates the loading rate effect on the pullout behavior of single fibers embedded ultra-high performance concrete. The loading rates range from 0.025 mm/s (quasi-static) to 25 mm/s (seismic). The experimental program is divided into two subprograms as follows: 1) investigating the effect of fiber type on the loading rate sensitive behavior for four types of high strength steel fibers, and 2) investigating the effect of fiber embedment angle on loading rate sensitive behavior for three fiber embedment angles. Based on the knowledge that crack formation is strain rate sensitive, the hypothesis is proposed that the formation of micro-splitting cracks and the damage of cement-based matrix in the fiber tunnel are the main reason for the loading rate sensitivity of singly pulled out fibers. Conclusions are summarized as follows:

1. Among the four fiber types investigated, HH-fiber (half-end hooked) exhibit strongest loading rate dependence with respect to maximum pull-out load and induced fiber tensile stress, followed by S-fiber (straight, small diameter), T-fiber (twisted) and SH-fiber (straight fibers with same diameter as HH-fibers). The DIFs at a pull-out rate of 25 mm/s are 1.28, 1.19, 1.14, and 1.01, respectively.
2. Among the four fiber types, T-fiber series exhibit strongest loading rate dependence with respect to pull-out energy and equivalent bond strength, followed by HH-fiber, S-fiber, and SH-fiber series. The DIFs at a pull-out rate of 25 mm/s are 1.43, 1.24, 1.03, and 0.95, respectively.
3. The loading rate sensitivity of HH-fiber and T-fiber can be primarily explained by the pullout mechanism and the proposed split cracking hypothesis. During pullout potential micro split cracking is generated in the local zone around end-hook of H-fiber or along the T-fiber. Crack inertia effects could lead to loading rate sensitivity during pullout.
4. The slight loading rate sensitivity of S-fibers embedded in UHPC might be attributed to matrix abrasion, fiber surface damage and minimal fiber end anchorage. No noticeable loading rate effect on straight SH-fibers of larger diameter (0.38 mm) embedded in UHPC has been observed.
5. Comparing the load rate sensitive behavior between SH-fiber (d = 0.38 mm) and S-fiber (d = 0.2 mm) suggests that decrease in diameter increase the rate sensitivity of straight fiber embedded in ultra-high strength matrix.
6. Fiber embedment angles influence the loading rate effect on pullout behavior. In this research a 20° embedment angle increases the pullout resistance by more than 20% and shows a promising effect on improving the pullout behavior at seismic loading rate.

Acknowledgement

This research has been supported by a fellowship within the Postdoctoral-Programme of the German Academic Exchange Service (DAAD), the University of Michigan and the University of Connecticut. Special appreciation is sent to Prof. Naaman and Prof. El-Tawil, who provided excellent research conditions for acquiring the experimental data at the University of Michigan. The writers also like to acknowledge the following companies for providing material free of charge: Bekaert, Elkem Materials and Lehigh Cement Company.

References

[1] A.E. Naaman, H. Najim, Bond-slip mechanisms of steel fibers in concrete, ACI Mater. J. (1991) 135–145. No 2.
[2] N. Banthia, A study of some factors affecting the fiber-matrix bond in steel fiber reinforced concrete, Can. J. Civ. Eng. (1990) 610–620. No.17.
[3] C. Sujiravorakul, Development of High Performance Fiber Reinforced Cement Composites Using Twisted Polygonal Steel Fibers, PhD thesis, University of Michigan, Ann Arbor, MI, 2001.
[4] P. Robins, S. Austin, P. Jones, Pull-out behavior of hooked steel fibers, Mater. Struct. 35 (2002) 434–442.
[5] D. Kim, S. El-Tawail, A.E. Naaman, Loading rate effect on pullout behavior deformed steel fibers, ACI Mater. J. (2008) 576–584. No. 6.
[6] V.M.C.F. Cunha, J.A.O. Barros, J.M. Sena-Cruz, Pullout behavior of steel fibers in self-compacting concrete, J. Mater. Civ. Eng. ASCE (2010) 1–9. No.1.
[7] K. Wille, A.E. Naaman, Pullout behavior of high-strength steel fibers embedded in ultra-high performance concrete, ACI Mater. J. (2012) 479–487. No. 4.
[8] U. Gokoz, A.E. Naaman, Effect of strain rate on the pull-out behavior of fibers in mortar, Int. J. Cem. Compos. (1981) 187–202. No.3.
[9] V. Bindiganavile, N. Banthia, Impact response of the fiber-matrix bond in concrete, Can. J. Civ. Eng. (2005) 924–933. No.32.
[10] N. Banthia, J.-F. Trottier, Deformed steel fiber-cementitious matrix bond under impact, Cem. Concr. Res. 21 (1991) 158–168.
[11] T. Abu-Lebdeh, S. Hamoush, B. Zornig, Rate Effect on Pullout Behavior of Steel Fibers Embedded in Very-High Strength Concrete, Am. J. Eng. Appl. Sci. 3 (No. 2) (2010) 454–463.
[12] J.M. Alwan, A.E. Naaman, P. Guerrero, Effect of Mechanical Clamping on the Pull-Out Response of Hooked Steel Fibers Embedded in Cementitious Matrices, Concr. Sci. Eng. 1 (1999) 15–25.
[13] K. Wille, Concrete strength dependent pull-out behaviour of deformed steel fibers, in: Proceedings of BEFIB2012 – 8th RILEM International Symposium on Fibre Reinforced Concrete: Challenges and Opportunites. Guimares. Portugal. September 19-21, 2012, pp. 69–70 (Full article on CD).
[14] J. Smith, G. Cusatis, D. Pelessone, E. Landis, J. O'Daniel, J. Baylot, Discrete modeling of ultra-high-performance concrete with application to projectile penetration, Int. J. Impact Eng. 65 (2014) 13–32.
[15] K. Wille, A.E. Naaman, Effect of ultra-high-performance concrete on pullout behavior of high-strength brass-coated straight fibers, ACI Mater. J. (2013) 451–462. No. 4.
[16] K. Wille, A.E. Naaman, G.J. Parra-Montesinos, Ultra-high performance concrete with compressive strength exceeding 150 MPa (22kis): a simpler way, ACI Mater. J. (2011) 46–54. No 1.
[17] K. Wille, A.E. Naaman, S. El-Tawil, G.J. Parra-Montesinos, Ultra-high performance concrete and fiber reinforced concrete: achieving strength and ductility without heat treatment, Mater. Struct. 45 (No. 3) (2012) 309–324.
[18] K. Wille, D. Kim, A.E. Naaman, Strain-hardening UHP-FRC with low fiber contents, Mater. Struct. 44 (No. 3) (2011) 583–598.
[19] K. Wille, S. El-Tawil, A.E. Naaman, Properties of strain hardening ultra-high performance fiber reinforced concrete (UHP-FRC) under direct tensile loading, Cem. Concr. Compos. 48 (2014) 53–66.
[20] Zhong, R., Wille, K., Equal Arc Segment Method for Averaging Data Plots Exemplified for Averaging Stress versus Strain Curves of Pervious Concrete, ASCE Journal of Materials in Civil Engineering, 10.1061/(ASCE)MT.1943-5533.0001345, 04015071.
[21] V.C. Li, Y. Wang, S. Backer, Effect of inclining angle, bundling and surface treatment on synthetic fiber pull-out from a cement matrix, Composites (1990) 132–140. No. 2.
[22] Y. Lee, Su-Tae Kang, Jin-Keun Kim, Pullout behavior of inclined steel fiber in an ultra-high strength cementitious matrix, Constr. Build. Mater. (2010) 2030–2041. No. 24.